The Journal of Eukaryotic Microbiology

ISOP Published by the International Society of Protistologists

Journal of Eukaryotic Microbiology ISSN 1066-5234

ORIGINAL ARTICLE

The *Trypanosoma brucei* RNA-Binding Protein TbRRM1 is Involved in the Transcription of a Subset of RNA Pol II-Dependent Genes

Carolina P. Bañuelos[1], Gabriela V. Levy[1], Analía G. Níttolo, Leandro G. Roser, Valeria Tekiel & Daniel O. Sánchez

Instituto de Investigaciones Biotecnológicas, Universidad Nacional de San Martín (IIB-UNSAM) – Consejo Nacional de Investigaciones Científicas y Técnicas (CONICET), 25 de Mayo y Francia, San Martín, Buenos Aires, Argentina

Keywords
Chromatin remodeling; epigenetic regulation; RNA Polymerase II; transcription elongation; *trans*-splicing.

Correspondence
D. O. Sánchez and G. V. Levy, Laboratorio de Genética Molecular de Trypanosomátidos, Instituto de Investigaciones Biotecnológicas, Universidad Nacional de San Martín (IIB-UNSAM), 25 de Mayo y Francia, San Martín, Buenos Aires, Argentina
Telephone number: +(5411)4006-1500;
FAX number: +(5411)4006-1559;
e-mails: dsanchez21@gmail.com; dsanchez@iib.unsam.edu.ar (D.O.S.) and gvlevy@gmail.com; glevy@iib.unsam.edu.ar (G.V.L.)

[1]These authors contributed equally to this work.

Received: 19 October 2018; revised 11 January 2019; accepted January 25, 2019.

doi:10.1111/jeu.12716

ABSTRACT

It has been long thought that RNA Polymerase (Pol) II transcriptional regulation does not operate in trypanosomes. However, recent reports have suggested that these organisms could regulate RNA Pol II transcription by epigenetic mechanisms. In this paper, we investigated the role of TbRRM1 in transcriptional regulation of RNA Pol II-dependent genes by focusing both in genes located in a particular polycistronic transcription unit (PTU) and in the monocistronic units of the *SL-RNA* genes. We showed that TbRRM1 is recruited throughout the PTU, with a higher presence on genes than intergenic regions. However, its depletion leads both to the decrease of nascent RNA and to chromatin compaction only of regions located distal to the main transcription start site. These findings suggest that TbRRM1 facilitates the RNA Pol II transcriptional elongation step by collaborating to maintain an open chromatin state in particular regions of the genome. Interestingly, the *SL-RNA* genes do not recruit TbRRM1 and, after *TbRRM1* knockdown, nascent *SL-RNAs* accumulate while the chromatin state of these regions remains unchanged. Although it was previously suggested that TbRRM1 could regulate RNA Pol II-driven genes, we provide here the first experimental evidence which involves TbRRM1 to transcriptional regulation.

TRYPANOSOMA brucei, the causative agent of sleeping sickness in humans and Nagana in cattle, has long been responsible for a significant proportion of global morbidity and economic loss threatening 70 millions of people in 36 countries in Africa (Simarro et al. 2012). Despite the number of new cases has dropped significantly thanks to sustained and coordinated large-scale control efforts, the disease is still endemic in some regions of Africa (Buscher et al. 2017). This early branching eukaryote has an atypical genome organization with its protein-coding genes generally organized in long polycistronic transcription units (PTU) across 11 mega-chromosomes (Melville et al. 1998). For this reason, the generation of individual mRNAs from immature transcripts requires the *trans*-splicing of a 39-nt-spliced leader (SL), which is common to all mature mRNAs (Liang et al. 2003; Vanhamme and Pays 1995). The non-conventional genome arrangement and the polycistronic transcription of functionally unrelated genes, has therefore led to assume that transcription is an uncontrolled process and that gene expression is regulated mainly post-transcriptionally at the level of mRNA degradation, translation (Clayton and Shapira 2007; Kramer and

Carrington 2011) or maturation (Nilsson et al. 2010; Siegel et al. 2011). However, it has been proposed that the expression of stage-specific proteins could be regulated at the chromatin structure level. For instance, in the bloodstream stage, the actively transcribed bloodstream expression site (BES) is depleted of nucleosomes, while histone H3 is most enriched in silenced *VSG* genes and in nontranscribed minichromosome regions (Figueiredo and Cross 2010; Stanne and Rudenko 2010). Similarly, coding regions of *rRNA* genes are depleted of nucleosomes as well as promoter regions of RNA Polymerase (Pol) I and Pol III-transcribed genes, or the only well-characterized SL-RNA Pol II promoter (Stanne and Rudenko 2010). In addition, chromatin remodeling of BES is involved in successful antigenic switching, thus allowing the parasite to evade the host immune system (Aresta-Branco et al. 2016). Collectively, these reports indicate that transcriptionally active genes could be found depleted of nucleosomes allowing a more permissive chromatin structure, while silenced or nontranscribed genes are most enriched of nucleosomes leading to a more compacted chromatin. This epigenetic transcription regulation has been involved in the expression of genes with well-defined promoters, while little is known about how chromatin accessibility can regulate Pol II polycistronic transcription initiation since no evidence of obvious nucleosome depletion has been found in transcription start sites (TSSs) (Maree et al. 2017; Wedel et al. 2017).

Several epigenetic markers have been described to define PTUs in *T. brucei*. Trimethylated histone H3 (Wright et al. 2010), acetylated histone H4 (H4K10ac), histone variants H2AZ and H2BV or the bromodomain factor BDF3 (Siegel et al. 2009) were shown to be enriched specifically at TSSs. Furthermore, a recent study has shown that the 5′ end of H2AZ-enriched regions are the primary sites of RNA Pol II initiation (Wedel et al. 2017). On the contrary, the β-D-glucosyl-hydroxymethyluracil modification known as base J (Reynolds et al. 2014) and histone variants H3V (Reynolds et al. 2016; Schulz et al. 2016) and H4V (Siegel et al. 2009) are enriched at RNA Pol II transcription termination sites. Moreover, in *T. cruzi* it has been shown that the presence of base J at Pol II promoter regions could regulate transcription initiation altering the chromatin structure (Ekanayake and Sabatini 2011). Together these studies suggest that chromatin organization plays a key role in defining the trypanosome transcription units and it might somehow participate in its transcriptional regulation.

Post-transcriptional regulation in trypanosomes involves different RNA-binding proteins (RBPs) (reviewed in (Clayton 2013, 2014)), including the Serine-Arginine (SR) and SR-related families. Several SR proteins exist in *T. brucei*, among them: TSR1 (Ismaili et al. 1999) and TSR1IP (Ismaili et al. 2000), and one SR-related protein, TbRRM1 (RNA-binding protein RRM1) (Manger and Boothroyd 1998). TSR1 and TSR1IP have been shown to be involved in *cis* and *trans*-splicing, as well as in the regulation of mRNA stability of a subset of transcripts and in rRNA processing (Gupta et al. 2014). Recently, it has been shown that TbRRM1 is involved in cell cycle regulation (Levy et al. 2015), and both chromatin structure and transcriptome modulation (Naguleswaran et al. 2015).

In the present work, we show that TbRRM1 plays a role in RNA Pol II transcriptional regulation since its depletion downregulates transcription of a subset of protein-coding genes. Analysis of a particular PTU showed that TbRRM1 is recruited along the entire unit, with higher presence on genes than on intergenic regions (IRs). In addition, only the regions located further downstream of the main divergent strand switch region (dSSR) are both transcriptionally affected and more compacted after TbRRM1 depletion; thus suggesting that TbRRM1 could play a role in RNA Pol II elongation by modulating the chromatin structure. Even though it was previously suggested that TbRRM1 could regulate RNA Pol II-driven genes, we provide here the first experimental evidence linking TbRRM1 with transcriptional regulation.

MATERIALS AND METHODS

Parasite culture and RNAi induction

Trypanosoma brucei procyclic cells, strain 29-13 transfected with p2T7- 5′UTR-TbRRM1 (Levy et al. 2015), were maintained in SDM-79 (Life Technologies, Carlsbad, CA) cell culture media as described previously (Montagna et al. 2006) in the presence of hygromycin (50 μg/ml), G418 (10 μg/ml), and phleomycin (2.5 μg/ml) (Invivogen, San Diego, CA). Cell density was determined daily using a Neubauer hemocytometer. Cells were grown exponentially to induce RNAi in procyclic forms at a starting density of 1×10^6 parasites/ml and maintained in the absence or presence of 1 μg/ml tetracycline (TET) (Invivogen) for at least 24 h.

Heat shock and sinefungin assay

Parasite from 20 ml cultures (~5×10^6 cells/ml) at 28 °C were added to one volume (20 ml) of SDM-79 at 53 °C as previously described (Kramer et al. 2008) and then incubated at 42 °C in a water bath for 30 min. The control cells were also incubated for 30 min at 28 °C (Fig. S5B). Sinefungin (2 μg/ml, Sigma, Saint Louis, MO) was used for 30 min or 3 h at 28 °C (Kramer et al. 2012). Following incubation, cells were washed and processed for RNA extraction. Three biological replicates were performed on different days (Fig. S5C).

Biotin-CTP incorporation assay

Assays reactions were carried out as described previously (Ullu and Tschudi 1990) with minor modifications. Briefly, 7.5×10^8 parasites were grown in exponential phase in the presence or absence of TET. As transcriptional negative control, parasites were incubated with Actinomycin D (Act-D) (10 μg/ml, Sigma) for 20 min (Fig. S3). After two washes with SDM-79 lacking fetal bovine serum (FBS), cells were resuspended and washed again with buffer A containing Sucrose (150 mM), KCl (20 mM), $MgCl_2$ (3 mM), Hepes-KOH pH = 7.9 (20 mM), DTT (1 mM), Leupeptin (10 μg/ml). Parasites were resuspended at

1.2×10^9 cells/ml and separated in 400 μl aliquots. After 5 min on ice, cells were permeabilized with Lysolecithin (500 μg/ml, Sigma) for 1 min on ice. Permeabilization was stopped by adding two volumes of Buffer A at room temperature. After washing, biotin-CTP incorporation assay was initiated by adding one volume of Buffer B 2× (2 mM ATP, 1 mM GTP, 1 mM UTP, 75 mM Sucrose, 20 mM KCl, 3 mM $MgCl_2$, 1 mM DTT, 10 μg/ml Leupeptin, 25 mM creatine phosphate, 0.6 mg/ml creatine kinase). To experimental samples biotin-14-CTP (0.5 mM) was added while CTP (0.5 mM) was added to control samples. Parasites were incubated at 28 °C for 20 min and the reaction was stopped by adding DNAse RQ1 (10 U, Promega, Madison, WI). Total RNA was extracted by Trizol according to manufacturer instruction. Biotinylated RNA was purified by magnetic Dynabeads (Invitrogen, Carlsbad, CA). Biotin incorporation assays were validated by RTqPCR and PCR (Fig. S7D, E, respectively).

Bromo uridine incorporation—FACS

Bromouridine (BrU) incorporation was assayed essentially as described above. Assays were performed in the presence of BrU (0.5 mM, Sigma) or UTP at 28 °C for 10 min in parasites from TET− and TET+ cultures. Additionally, cells from TET− or TET+ cultures incubated with Act-D (10 μg/ml) for 20 min were used as transcriptional negative control. The reaction was stopped by 4% paraformaldehyde (PFA) fixation. BrU-RNA molecules were detected with 1:500 anti-BrdU (clone BU:33, Sigma) and an Alexa Fluor 488-conjugated goat anti-mouse (Molecular Probes, Eugene, OR) was used 1:1000 as secondary antibody. Data were acquired with a Partec CyFlow Space cytometer using FL-1 detector and analyzed with FlowJo software. A total of 50,000 events were acquired in the region previously established as corresponding to *T. brucei* procyclic cells, based on forward (FSC) and side (SSC) scatter channels. Quantification of BrU+ cells was performed from two-parameter dot plot (FL-1 vs. FSC) with a quadrant marker obtained from UTP-incorporation assay cells considering TET− BrU+ cells as 100% (Table S2).

RNA extraction and reverse transcription

Total RNA was isolated from TET− and TET+ cultures with Trizol Reagent according to manufacturer's instructions (Life Technologies) and RNA integrity was evaluated by agarose gel electrophoresis. Finally, samples were incubated with DNAse RQ1 (Promega) followed by chloroform extraction and ethanol precipitation. First strand cDNA was synthesized from total or purified RNA samples using Superscript II reverse transcriptase and random hexamers, according to manufacturer's instructions (Life Technologies).

FAIRE technique

Formaldehyde-assisted isolation of regulatory elements (FAIRE) was performed essentially as described previously (Pena et al. 2014). In brief, a total of 1.2×10^8 cells were fixed for 10 min in 1% PFA in PBS. An external DNA spike consisting of the vector pGR86 (gently given by Dr. Antonio M. Estévez) containing a luciferase gene was added to the samples prior to sonication. DNA was sonicated with a Branson Sonifier 450 for 15 min total (30 s On-Off cycles), such that the resulting chromatin fragments averaged 500 bp in length. Sonicated chromatin was submitted to two consecutive phenol-chloroform extractions, and DNA was ethanol precipitated in the presence of linear polyacrylamide as carrier, resuspended in TE buffer, and treated with RNAse A (100 μg/ml, Sigma) at 37 °C for 1 h and with proteinase K (200 μg/ml, Sigma) at 55 °C for 3 h. Quantification of the FAIRE and total DNA samples were performed by real-time quantitative PCR (qPCR).

Chromatin immunoprecipitation (ChIP)

Chromatin immunoprecipitation assay was performed as previously described (Stanne and Rudenko 2010). Briefly, DNA was cross-linked to protein using PFA as in FAIRE technique. Chromatin from 6×10^7 cell was used in each immunoprecipitation (IP) reaction. Lysate was incubated with anti-TbRRM1 or pre-immune mouse serum, overnight at 4 °C. Protein-DNA complexes were incubated with protein A-Sepharose CL-4B beads (GE Healthcare, Chicago, IL) for 2 h. DNA was eluted from beads using elution buffer containing 1% SDS and $NaHCO_3$ (0.1 M). Cross-linking was then reversed by adding NaCl to a final concentration of 325 mM and incubated at 65 °C overnight. DNA was then extracted using phenol-chloroform after RNAse A and proteinase K treatments. Each ChIP experiment was performed in triplicate and analyzed by qPCR. Results are expressed as the percent input method (% IP) calculated by the formula % IP = 100* 2(Cq (Adjusted input) − Cq (IP)).

RTqPCR and qPCR

Real time quantitative PCR (qPCR) or retrotranscription followed by qPCR (RTqPCR) were performed using Kapa Sybr Fast Universal Kit (Sigma) with primers described in Table S1A. For *trans*-splicing assays, forward primers were designed upstream the 5′ UTR (for precursor mRNAs) or at the SL miniexon (shared for all mature mRNAs), while a common reverse primer was designed downstream the 3′ splice site (3′ SS) of each analyzed gene (see Table S1B and Fig. S1). The reactions were carried out with the 7500 Real Time PCR System from Applied Biosystems. Unless otherwise indicated for the RNA abundance levels, samples were normalized to *18S rRNA*, which did not change significantly after TbRRM1 depletion (see Cq values in Fig. S7A). For transcriptional assays, *RPL10A/RPL30* genes (located on chromosomes 11 and 10, respectively) were previously validated as transcriptional controls by luciferase RNA external spike, since transcription levels did not change upon *TbRRM1* knockdown (Fig. S7B, C). Finally, FAIRE results were normalized to the luciferase DNA spike. The results were analyzed using LinReg (Ramakers et al. 2003) and REST (Pfaffl et al. 2002) programs.

Statistical analyses

Data from FAIRE, abundance of newly synthesized RNA and RNA levels were analyzed by means of the relation TET+/TET− using one-sample two-tailed Student *t*-test. ChIP results were analyzed comparing % IP vs. non-specific binding. The TbRRM1 distribution on genes vs. IRs was analyzed by two-tailed Student *t*-test with Welch's correction. Correlation analyses were performed among these values with the Pearson correlation coefficient with GraphPad Software.

RESULTS

Trans-splicing of genes downregulated by TbRRM1 depletion remains unaffected

Previously, it was reported that TbRRM1 is involved in both chromatin and transcriptome modulation (Naguleswaran et al. 2015). In order to know how TbRRM1 participates in these processes, we started to investigate transcription and splicing as it is well-known that both mechanisms are influenced by modifications of the chromatin structure (Jimeno-Gonzalez and Reyes 2016; Naftelberg et al. 2015). To know whether TbRRM1 depletion induces the downregulation of genes by affecting the *trans*-splicing process, we analyzed two genes, *TbNOP86*, which we have previously demonstrated that TbRRM1 depletion downregulates its expression (Levy et al. 2015) and the *60S ribosomal protein L38* gene, which is a neighbor of *TbNOP86*. To analyze *trans*-splicing, we determined by RTqPCR, the pre/mature mRNA ratio of both genes in TbRRM1-RNAi parasites treated or not with tetracycline (TET) (see schemes on Fig. 1 and Fig. S1, and Table S1B for primer details). This parasite line expresses an RNAi against the 5′UTR of TbRRM1 (Levy et al. 2015). To identify primary effects of TbRRM1 depletion, experiments were carried out at 24 h of TET addition, since it is the earliest time point at which both the TbRRM1 protein level is undetectable and the parasite growth curve remains almost unaltered (Levy et al. 2015). No changes were detected in pre/mature mRNA ratio in parasites depleted of TbRRM1 (TET+) relative to control parasites (TET−) for any of the analyzed transcripts, thus suggesting that the downregulation, induced by TbRRM1 depletion, was due to mechanisms other than *trans*-splicing (Fig. 1).

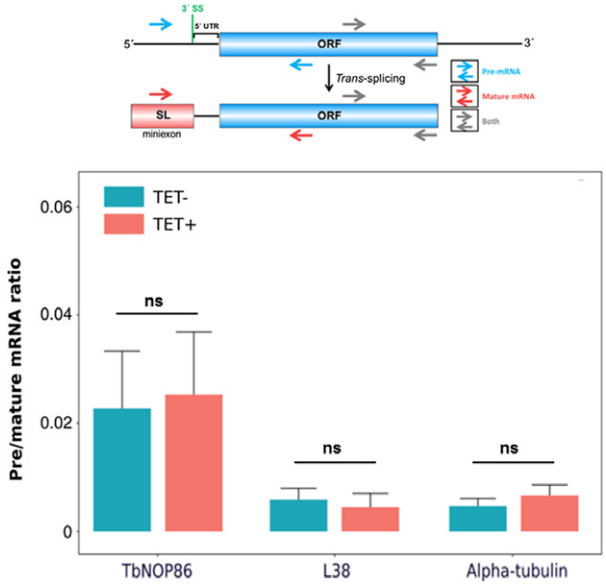

Figure 1 *Trans*-splicing remains unaffected in genes downregulated by *TbRRM1* knockdown. Precursor levels (pre-mRNA) of *TbNOP86* and *60S ribosomal L38 protein* were relativized to the mature mRNA assayed in TET− and TET+ cultures. No significant (ns) changes were observed comparing both conditions. The *alpha-tubulin* gene served as control as its steady-state mRNA level is not affected after TbRRM1 depletion (Naguleswaran et al. 2015). Upper scheme shows the experimental design and localization of primers (arrows) used for this assay (for more details see Fig. S1).

TbRRM1 knockdown downregulates transcription

Taken into account that the *trans*-splicing process was not affected, we decided to test whether *TbRRM1* knockdown induces a transcriptional defect. To this end, TET induced and uninduced TbRRM1-RNAi parasites were subjected to transcriptional assays in the presence of bromouridine (BrU) to label newly synthesized RNAs and analyzed by FACS. To control whether BrU was incorporated into RNA, parallel experiments were performed in the presence of Actinomycin D (Act-D) to inhibit transcription. The BrU+ parasite population was reduced by 41% after RNAi induction when compared to uninduced parasites (Fig. 2 and Table S2), thus suggesting an impairment in transcription after *TbRRM1* knockdown. The presence of Act-D in the transcriptional assays further decreased the BrU incorporation indicating that it was indeed incorporated into RNA transcripts.

TbRRM1 facilitates transcription of the PTU-TbNOP86

To further corroborate the previous finding, we decided to evaluate transcription of a set of genes that are downregulated by TbRRM1 depletion. Particularly, we focused on genes located in the PTU containing the gene *TbNOP86* (dubbed PTU-TbNOP86), because the mRNA abundance of this gene was among the most affected upon depletion of TbRRM1 (Levy et al. 2015). The PTU-TbNOP86 is an RNA Pol II-transcribed PTU located on the minus strand of chromosome 9 (www.tritrypdb.org) encompassing ~3.7 × 10^5 bp. First and last annotated genes of PTU-TbNOP86 were identified previously as Tb927.9.3170 and Tb9 27.9.1340, respectively (Kolev et al. 2010). Transcription of this PTU starts within a divergent strand switch region (dSSR) of ~4,300 bp located to the right of the PTU, from nucleotide 686,312 to 690,645 (defined by the region from the first base of the gene located in the minus strand to the first nucleotide of the gene located at the plus strand). This dSSR is surrounded by twin peaks of acetylated H4 histone (H4K10ac) and the histone variants H2AZ and H2BV, which signals TSSs (Siegel et al. 2009). There are

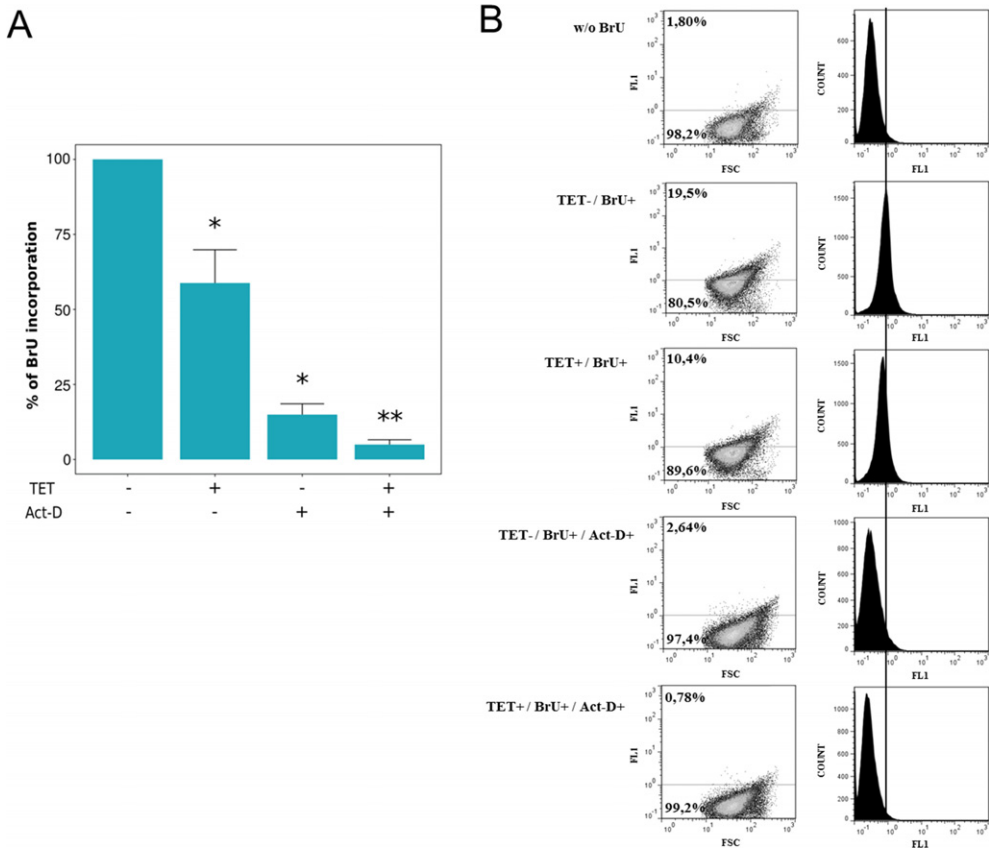

Figure 2 *TbRRM1* knockdown downregulates transcription. (**A**) Bromouridine (BrU) incorporation experiments assayed by FACS after 24 h silencing of *TbRRM1*. Percentage of BrU incorporation by parasites grown in the absence (TET−) or presence (TET+) of tetracycline. Error bars indicate the standard deviations around the mean from three independent experiments for Act-D− or two for Act-D+. Data were analyzed by one-sample Student *t*-test comparing results to the hypothetical value of 100. $*P < 0.05$, $**P < 0.01$. (**B**) Two-parameter dot plot (FL-1 vs. FSC) and FL-1 histograms from each experimental condition were obtained by FACS. Dot plots and histograms from TET− and TET+ cultures representative of independent biological replicates are shown. Act-D = actinomycin D.

also additional histone peaks located downstream indicating a putative internal TSS in this PTU (Fig. S2).

To evaluate transcription in this PTU, we carried out biotin-CTP incorporation assays on permeabilized parasites to label newly synthesized RNAs. The level of transcription in genes and intergenic regions (IRs), either proximal or distal to both TSSs, was analyzed by RTqPCR on biotin-labeled RNA from parasites depleted or not of TbRRM1. Analysis of the PTU showed that biotin-RNA levels were severely affected in the central part, while no changes, or a slightly but not significant increase was observed in regions closer to or within the dSSR, and at most regions located downstream the internal TSS (Fig. 3A). The presence of Act-D showed a significant decrease of the biotinylated RNA (Fig. S3). These data suggest that TbRRM1 might be implicated in transcription elongation rather than in the initiation step since only the regions of the PTU-TbNOP86 located distal to the dSSR were compromised after its knockdown.

In parallel, we also analyzed, in parasites depleted or not of TbRRM1, the RNA steady-state levels of the same genes and IRs shown in Fig. 3A. As shown in Fig. 3B, the RNA levels follow a pattern quite similar to the transcription one, suggesting that regulation of gene expression in the PTU-TbNOP86 could be mainly driven by transcriptional regulation. Supporting this finding we found a significant correlation between transcription levels and RNA abundance ($r = 0.672$, two-tailed *t*-test, $***P < 0.001$; Fig. S4A).

Next, we wanted to know whether TbRRM1 depletion also affects the level of newly synthesized *SL-RNA* which are also transcribed by the RNA Pol II (Gilinger and Bellofatto 2001). Interestingly, the abundance of labeled *SL-RNA* was slightly, but significantly, increased in parasites depleted of TbRRM1 (Fig. 3C), which correlated with increased *SL-RNA* levels (Fig. 3D and (Naguleswaran et al. 2015)). These results suggest that TbRRM1 might be involved in transcription repression of the *SL-RNA* genes, as depletion of TbRRM1 increased their transcription.

TbRRM1 depletion leads to chromatin condensation in the PTU-TbNOP86 but not in the *SL-RNA* genes

Taking into account that TbRRM1 depletion leads to transcription impairment (shown above), and its possible role as a chromatin modulator (Naguleswaran et al. 2015) we

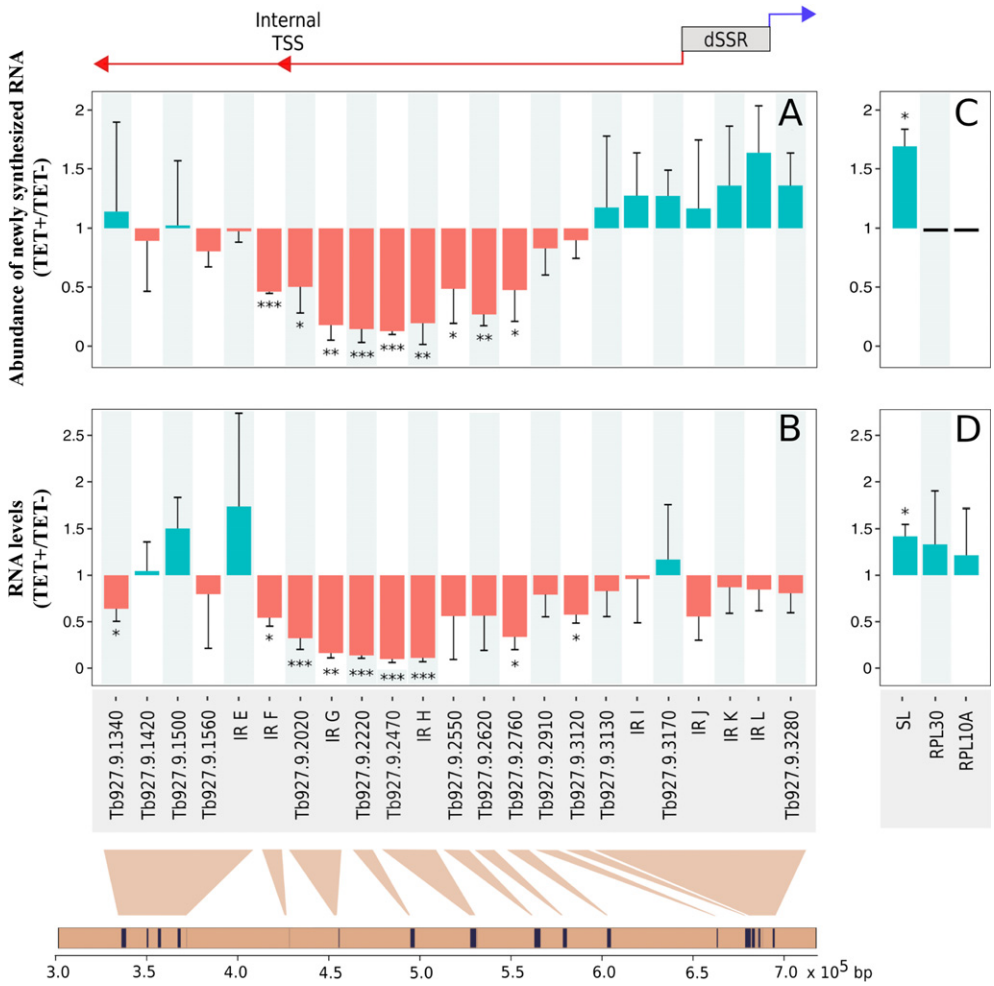

Figure 3 Analysis of transcription and RNA levels after *TbRRM1* knockdown. (**A**) Biotin-CTP incorporation experiments. The level of newly synthesized RNA was analyzed by RTqPCR on biotin-labeled RNA in the PTU-TbNOP86. (**B**) RNA steady-state levels of the same regions shown in A. (**C**) Analysis of *SL-RNA* genes and control genes *RPL10A* and *RPL30*. (**D**) RNA levels of the same genes analyzed in C. Data from the abundance of newly synthesized RNA assays were normalized to *RPL10A* and *RPL30* mRNA since its biotin-labeled mRNA levels did not change after TbRRM1 depletion, while results from RNA abundance were normalized to *18S rRNA*. The bars indicate the average of at least three independent biological replicates ± standard deviation. Data were analyzed by one-sample two-tailed Student *t*-test. $*P < 0.05$, $**P < 0.01$, $***P < 0.001$.

decided to evaluate the chromatin state in the PTU-TbNOP86 to know whether the transcriptional impairment on this PTU was due to chromatin compaction of this region. To this end, we took advantage of the Formaldehyde-Assisted Isolation of Regulatory Elements (FAIRE) technique (Giresi et al. 2007) to investigate nucleosome abundance. In the FAIRE technique the nucleosome-depleted or naked regions of the genome are recovered in the aqueous phase (soluble chromatin) after phenol:chloroform extraction of formaldehyde-cross-linked chromatin, then ethanol precipitated and the regions of interest are quantified by qPCR.

FAIRE results showed that TbRRM1 ablation induced the decrease of the soluble chromatin levels in the central region of this PTU compared to the dSSR (Fig. 4A). These results were further corroborated by chromatin immunoprecipitation (ChIP) of histone H3 (data not shown) and correlated with the abundance of newly synthesized RNA data shown in Fig. 3A ($r = 0.607$, two-tailed *t*-test, $**P < 0.01$; Fig. S4B), suggesting that lower levels of nascent RNAs could be the outcome of an impaired transcription due to a more closed chromatin structure (Moretti and Schenkman 2013; Zhou et al. 2007).

FAIRE analysis was also carried out in the genes *SL-RNA*, *RPL10A* and *RPL30* (Fig. 4B). The *SL-RNA* genes exhibited no differences in chromatin compaction after *TbRRM1* knockdown, thus suggesting that TbRRM1 is not involved in chromatin condensation of these genes. Interestingly, the *RPL10A* and *RPL30* genes whose transcription was not affected, showed a more compacted chromatin after TbRRM1 depletion, suggesting that expression of these genes is independent of the chromatin state induced by *TbRRM1* knockdown (compare Fig. 3C, 4B).

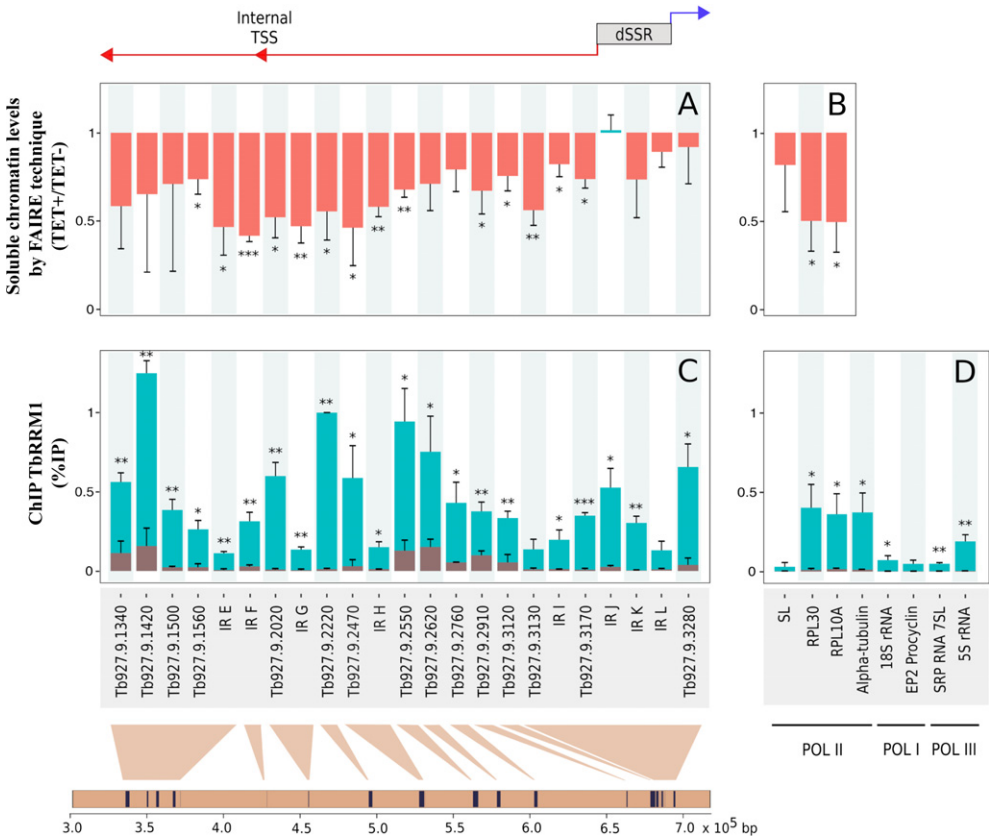

Figure 4 TbRRM1 binds to chromatin and its absence leads to chromatin compaction. (**A**) Chromatin structure analysis along the PTU-TbNOP86 in control (TET−) and in TbRRM1 depleted cells (TET+) by the FAIRE technique. (**B**) FAIRE analysis of *SL-RNA* genes and control genes *RPL10A* and *RPL30*. Data from FAIRE assays were normalized to an external luciferase DNA spike and analyzed by one-sample two-tailed Student *t*-test. (**C**) Distribution of TbRRM1determined by chromatin immunoprecipitation (ChIP) over selected regions of the PTU-TbNOP86 are shown as the % IP method (see Materials and Methods Section for details). (**D**) ChIP assay of the same genes analyzed in B and in other genomic regions transcribed by different polymerases. Gray overlapped bars show non-specific binding (pre-immune mouse serum) for each amplicon. The bars indicate the average of at least three independent biological replicates ± standard deviation. Data from TbRRM1-ChIP were analyzed by two-tailed Student *t*-test comparing to serum control. $*P < 0.05$, $**P < 0.01$, $***P < 0.001$.

TbRRM1 is preferentially recruited to protein-coding genes transcribed by RNA Pol II

FAIRE results showed that most genes and IRs located in the central region of the PTU-TbNOP86 increased its nucleosome abundance upon TbRRM1 depletion. To investigate whether TbRRM1 associates with chromatin, we assessed its presence along the PTU-TbNOP86 by ChIP. We observed the association of TbRRM1 with chromatin along the entire PTU, with a higher presence within genes than in the analyzed IRs, with the exception of the IRs located near both TSSs (Fig. 4C, 5). TbRRM1 highest occupancy was in the locus Tb927.9.1420, a hypothetical protein-coding gene, whose mRNA level, nascent RNA synthesis, and chromatin compaction remained unaffected after TbRRM1 depletion (Fig. 3A, B, 4A).

We also analyzed whether TbRRM1 binds to genes transcribed by different RNA polymerases. As seen in Fig 4D, TbRRM1 was recruited to *alpha-tubulin*, *RPL10A*, and *RPL30* genes and to a lesser extent to *18S rRNA* and the RNA Pol III-transcribed *5S rRNA* and *SRP RNA 7SL* genes. Interestingly, no interaction was detected with either the *SL-RNA* or the *EP2 Procyclin* gene, which is transcribed by the RNA Pol I. Altogether, these results suggest that TbRRM1 associates with chromatin, preferentially with protein-coding genes transcribed by RNA Pol II. Curiously, not all regions where TbRRM1 binds to chromatin are compacted in the absence of this protein (compare Fig. 4A, C). This finding was also supported by the lack of correlation between ChIP results and FAIRE data (Fig. S4C).

DISCUSSION

In trypanosomes, genes are mainly organized in long polycistronic units, whose mRNA precursors are co-transcriptionally processed. So it is normally assumed that regulation of gene expression in trypanosomes is at the post-transcriptional level where the fate of the mature

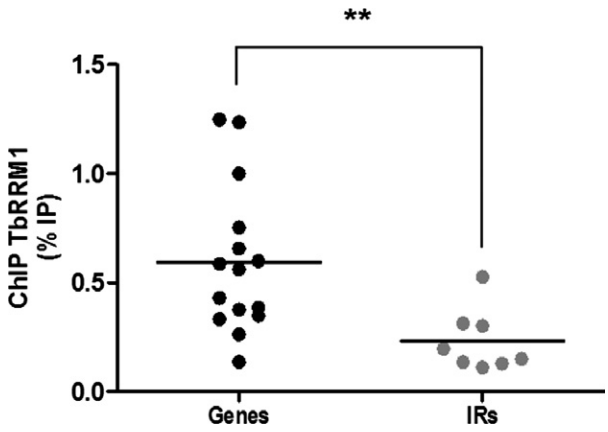

Figure 5 Levels of TbRRM1 chromatin association with genes vs. intergenic regions (IRs). Data from ChIP assays were pooled to compare TbRRM1 differential binding. Horizontal lines show the % IP mean and dots represent the mean of three independent ChIP assays. Data from TbRRM1-ChIP were analyzed by two-tailed Student *t*-test with Welch's correction. $^{**}P < 0.01$.

mRNA is exerted by RBPs that regulate mRNA stability and translatability among other processes (Clayton 2016). Interestingly, the codon usage also has a major impact on gene expression (de Freitas Nascimento et al. 2018) since it can control the mRNA stability and ribosome occupancy (Jeacock et al. 2018).

Up to now, transcriptional control seemed to be no relevant in trypanosomes. However, recently, several reports implicated various proteins in RNA Pol I and Pol III transcription regulation (Romero-Meza et al. 2017; Stanne et al. 2015), while little is known about the factors involved in transcriptional regulation of Pol II-driven genes. Interestingly, it has been shown that the spatial position of genes within a PTU can have a major impact in the control of gene expression. For instance, genes that are differentially regulated during the heat-shock response are differentially positioned within the PTUs, while upregulated genes tend to be located distal to the TSS, downregulated ones are located closer (Kelly et al. 2012).

In this paper, we investigated the gene expression regulation exerted by TbRRM1 in RNA Pol II-dependent genes. We focused on genes located in a particular PTU (PTU-TbNOP86), which is one of the two PTUs whereupon TbRRM1 depletion, the majority of genes are downregulated and none is upregulated (Naguleswaran et al. 2015), as well as the monocistronic transcription units of the *SL-RNA* genes. As the analysis of *TbNOP86* mRNA stability showed that it did not change upon TbRRM1 depletion (results not shown), we investigated the *trans*-splicing processing of *TbNOP86* and *L38* pre-mRNAs. Although it has been previously suggested that TbRRM1 does not play a role in global *trans*-splicing (Manger and Boothroyd 2001; Naguleswaran et al. 2015), it could be involved in the splicing processing of a small set of transcripts. We found that *trans*-splicing of both transcripts was unaffected (Fig. 1), thus showing that TbRRM1 is not involved in their processing. Interestingly, both pre-mRNA and mature mRNA levels diminished significantly in TbRRM1 depleted parasites, which suggested a transcriptional defect (Fig. S5A). To corroborate this finding, we carried out a transcriptional assay using the lysolecithin-permeabilized parasite model which allows the labeling of newly synthesized RNA maintaining a linear rate of nucleotide incorporation for 15–20 min (Ullu and Tschudi 1990). This system also supports an efficient *trans*-splicing process (Begolo et al. 2018; Ullu and Tschudi 1990).

To corroborate the transcriptional defect, we analyzed global transcription using BrU incorporation assays performed in living cells. These experiments showed a reduction of ~40% in the number of parasites incorporating BrU upon *TbRRM1* knockdown (Fig. 2 and Table S2). We then evaluated transcription levels and mRNA abundance of several genes belonging to the PTU-TbNOP86. As seen in Fig. 3A, transcription of most genes located in the central region of this PTU was downregulated in TbRRM1 depleted parasites. In addition, transcription levels and RNA abundance followed similar profiles along the PTU (compare Fig. 3A, B, see also Fig. S4A). These results suggest that at least in this PTU, transcription could be a major gene expression control point. Interestingly, transcription of genes proximal to the dSSR and the internal TSS remained mostly unaffected (Fig. 3A). Taken together, these results suggest that TbRRM1 is involved in the RNA Pol II transcription elongation phase, as only transcription of the central region of the PTU-TbNOP86 was compromised, but not near both ends, where TSSs are located. Interestingly, SR proteins, such as the mammalian splicing factor SRSF2 (previously called SC35), have already been linked to transcriptional elongation regulation (Jeong 2017). It has been established that SRSF2 has an early function in gene expression facilitating the recruitment of essential transcription elongation factors at gene promoters, causing the release of paused RNA Pol II (Ji et al. 2013; Lin et al. 2008).

It is well known that the degree of chromatin compaction influences transcription (Moretti and Schenkman 2013; Zhou et al. 2007) and vice versa (Berger 2007; Perales and Bentley 2009). Our FAIRE and transcriptional results also support this knowledge for protein-coding genes transcribed by the RNA Pol II in *T. brucei*. Indeed, depletion of TbRRM1 induced both chromatin compaction and transcription inhibition of most genes located in the central region of the PTU-TbNOP86, while the regions located within the dSSR, where there is no chromatin compaction, transcription was unaffected (see Fig. 3A, 4A).

In order to characterize the presence of TbRRM1 along the PTU-TbNOP86, we performed ChIP assays using formaldehyde-cross-linked chromatin and anti-TbRRM1 antibodies followed by qPCR. TbRRM1 was recruited to all regions within this PTU, although in higher amounts on genes than IRs indicating binding preferences and a non-uniform presence of TbRRM1 protein in this gene array (Fig. 4C, 5). Interestingly, ChIP results do not correlate with either FAIRE or transcriptional data (Fig. S4C, D),

thus suggesting that the regions recruiting TbRRM1 could be compacted or not upon TbRRM1 depletion. For instance, the region of the dSSR recruits TbRRM1, but in its absence, this region is not differentially compacted (Fig. 4A, C) and transcription is not affected (Fig 3A). On the contrary, the central region of this PTU, which also recruits TbRRM1, is compacted and transcription is repressed following TbRRM1 depletion. Together, these results suggest that additional factor(s) play an important role in chromatin condensation induced by *TbRRM1* knockdown.

It has previously shown that depletion of TbRRM1 upregulates the levels of approximately 300 transcripts (Naguleswaran et al. 2015), among them, a polyadenylated version of the *SL-RNA*, while the levels of regular *SL-RNA* remained unchanged. Here, we also observed a slightly, but significant increase in the *SL-RNA* levels (Fig. 3D), which may be the outcome of transcriptional upregulation of the *SL RNA* genes (Fig. 3C). Polyadenylation of the *SL-RNA* transcript has been previously reported in *T. brucei* (Pelle and Murphy 1993), as well as in *Leishmania* (Lamontagne and Papadopoulou 1999). In *Leishmania*, it was shown that polyadenylated *SL-RNA* forms bear in its 3′-end an additional 15-nucleotide sequence compared to regular *SL-RNA* forms, thus suggesting the use of an alternative maturation site, which might be the outcome of the RNA Pol II pausing further downstream. In this context, it is tempting to speculate that in *T. brucei*, TbRRM1 may be involved in regulating transcription-elongation and/or -termination steps of the *SL-RNA*. So, depletion of this protein may result in transcription dysregulation allowing the production of longer *SL-RNA* transcripts, which would then be polyadenylated. We also found that *SL-RNA* transcription units do not recruit TbRRM1 and that there is no difference in chromatin compaction after *TbRRM1* knockdown (Fig. 4B, D), thus suggesting that TbRRM1 does not have a role in chromatin regulation of these transcription units. This might be related to the deficiency of nucleosomes in the *T. brucei SL-RNA* genes and promoters ((Figueiredo and Cross 2010) and our unpublished results), as seen before in *Leishmania tarentolae* (Hitchcock et al. 2007). So it appears that TbRRM1 has different roles, behaving, in this case, as a negative transcriptional regulator of these monocistronic transcription units although probably independent of its role in chromatin remodeling. Interestingly, it has been recently shown that TbMAF1, a negative regulator of RNA Pol III transcription, also downregulates transcription of *SL-RNA* genes (Romero-Meza et al. 2017). Thus, it seems that multiple negative regulators participate in the transcriptional control of this important molecule in trypanosomes.

It has previously been shown by an RNA-seq analysis that TbRRM1 depletion decreases the abundance of about one-third of the *T. brucei* transcriptome (Naguleswaran et al. 2015). Among them, we found several genes involved in transcription, such as the transcription elongation factor *TFIIS1* (Uzureau et al. 2008) and homologues of the three subunits identified in *T. brucei* belonging to the RNA polymerase-associated factor (PAF) complex (Ouna et al. 2012), which has recently been shown to interact with the RNA Pol II (Srivastava et al. 2017). Therefore, it is tempting to speculate that downregulation of both, the PAF complex and the transcription elongation factor *TFIIS1*, may result in transcription elongation impairment as we showed in the PTU-TbNOP86 (Fig. 3A). However, we found by RTqPCR that the mRNA abundance of members of the PAF complex, as well as, the *TFIIS1* elongation factor did not change after 24 h of *TbRRM1* knockdown (Fig. S6), thus favoring the idea that chromatin condensation and transcription defects are primary consequences of TbRRM1 depletion.

In summary, our data suggest that TbRRM1 has different roles in transcriptional regulation of RNA Pol II transcription units. On one hand, it binds preferentially to genes facilitating transcription elongation of a subset of protein-coding genes by collaborating to maintain an open chromatin state. On the other hand, it negatively regulates transcription of the *SL-RNA* genes, independently of its role as chromatin remodeler.

Finally, although it has been long thought that RNA Pol II transcriptional regulation does not operate in these organisms, recent reports have suggested that trypanosomes could regulate RNA Pol II transcription by epigenetic mechanisms (Ekanayake and Sabatini 2011; Reynolds et al. 2016; Stanne and Rudenko 2010). Results reported in this paper present the first experimental evidence showing that the RBP TbRRM1 plays a key role in RNA Pol II transcriptional regulation in *T. brucei*.

ACKNOWLEDGMENTS

Authors want to thank Dr. Raul Cosentino and Dr. Nicolai Siegel for providing ChIP-seq raw data for histones H2AZ, H2BV, and H4K10ac and also to Dr. Antonio Estévez for supplying the pGR86 vector. GVL, VT, and DOS are Career Investigators from CONICET. This work was supported by Agencia Nacional de Promoción Científica y Tecnológica, (ANPCyT, Argentina, PICT 2014-0879 to DOS) and by the Consejo Nacional de Investigaciones Científicas y Técnicas (CONICET, Argentina).

CONFLICT OF INTEREST

The authors have declared that no competing interest exists.

LITERATURE CITED

Aresta-Branco, F., Pimenta, S. & Figueiredo, L. M. 2016. A transcription-independent epigenetic mechanism is associated with antigenic switching in *Trypanosoma brucei*. *Nucleic Acids Res.*, 44:3131–3146.

Begolo, D., Vincent, I. M., Giordani, F., Pohner, I., Witty, M. J., Rowan, T. G., Bengaly, Z., Gillingwater, K., Freund, Y., Wade, R. C., Barrett, M. P. & Clayton, C. 2018. The trypanocidal benzoxaborole AN7973 inhibits trypanosome mRNA processing. *PLoS Pathog.*, 14:e1007315.

Berger, S. L. 2007. The complex language of chromatin regulation during transcription. *Nature*, 447:407–412.

Buscher, P., Cecchi, G., Jamonneau, V. & Priotto, G. 2017. Human African trypanosomiasis. *Lancet*, 390:2397–2409.

Clayton, C. 2013. The regulation of trypanosome gene expression by RNA-binding proteins. *PLoS Pathog.*, 9:e1003680.

Clayton, C. E. 2014. Networks of gene expression regulation in *Trypanosoma brucei*. *Mol. Biochem. Parasitol.*, 195:96–106.

Clayton, C. E. 2016. Gene expression in kinetoplastids. *Curr. Opin. Microbiol.*, 32:46–51.

Clayton, C. & Shapira, M. 2007. Post-transcriptional regulation of gene expression in trypanosomes and leishmanias. *Mol. Biochem. Parasitol.*, 156:93–101.

de Freitas Nascimento, J., Kelly, S., Sunter, J. & Carrington, M. 2018. Codon choice directs constitutive mRNA levels in trypanosomes. *Elife*, 7:e32467.

Ekanayake, D. & Sabatini, R. 2011. Epigenetic regulation of polymerase II transcription initiation in *Trypanosoma cruzi*: modulation of nucleosome abundance, histone modification, and polymerase occupancy by O-linked thymine DNA glucosylation. *Eukaryot. Cell*, 10:1465–1472.

Figueiredo, L. M. & Cross, G. A. 2010. Nucleosomes are depleted at the VSG expression site transcribed by RNA polymerase I in African trypanosomes. *Eukaryot. Cell*, 9:148–154.

Gilinger, G. & Bellofatto, V. 2001. Trypanosome spliced leader RNA genes contain the first identified RNA polymerase II gene promoter in these organisms. *Nucleic Acids Res.*, 29:1556–1564.

Giresi, P. G., Kim, J., McDaniell, R. M., Iyer, V. R. & Lieb, J. D. 2007. FAIRE (Formaldehyde-Assisted Isolation of Regulatory Elements) isolates active regulatory elements from human chromatin. *Genome Res.*, 17:877–885.

Gupta, S. K., Chikne, V., Eliaz, D., Tkacz, I. D., Naboishchikov, I., Carmi, S., Waldman Ben-Asher, H. & Michaeli, S. 2014. Two splicing factors carrying serine-arginine motifs, TSR1 and TSR1IP, regulate splicing, mRNA stability, and rRNA processing in *Trypanosoma brucei*. *RNA Biol.*, 11:715–731.

Hitchcock, R. A., Thomas, S., Campbell, D. A. & Sturm, N. R. 2007. The promoter and transcribed regions of the Leishmania tarentolae spliced leader RNA gene array are devoid of nucleosomes. *BMC Microbiol.*, 7:44.

Ismaili, N., Perez-Morga, D., Walsh, P., Cadogan, M., Pays, A., Tebabi, P. & Pays, E. 2000. Characterization of a *Trypanosoma brucei* SR domain-containing protein bearing homology to cis-spliceosomal U1 70 kDa proteins. *Mol. Biochem. Parasitol.*, 106:109–120.

Ismaili, N., Perez-Morga, D., Walsh, P., Mayeda, A., Pays, A., Tebabi, P., Krainer, A. R. & Pays, E. 1999. Characterization of a SR protein from *Trypanosoma brucei* with homology to RNA-binding cis-splicing proteins. *Mol. Biochem. Parasitol.*, 102:103–115.

Jeacock, L., Faria, J. & Horn, D. 2018. Codon usage bias controls mRNA and protein abundance in trypanosomatids. *Elife*, 7: e32496.

Jeong, S. 2017. SR proteins: binders, regulators, and connectors of RNA. *Mol. Cells*, 40:1–9.

Ji, X., Zhou, Y., Pandit, S., Huang, J., Li, H., Lin, C. Y., Xiao, R., Burge, C. B. & Fu, X. D. 2013. SR proteins collaborate with 7SK and promoter-associated nascent RNA to release paused polymerase. *Cell*, 153:855–868.

Jimeno-Gonzalez, S. & Reyes, J. C. 2016. Chromatin structure and pre-mRNA processing work together. *Transcription*, 7:63–68.

Kelly, S., Kramer, S., Schwede, A., Maini, P. K., Gull, K. & Carrington, M. 2012. Genome organization is a major component of gene expression control in response to stress and during the cell division cycle in trypanosomes. *Open Biol.*, 2:120033.

Kolev, N. G., Franklin, J. B., Carmi, S., Shi, H., Michaeli, S. & Tschudi, C. 2010. The transcriptome of the human pathogen *Trypanosoma brucei* at single-nucleotide resolution. *PLoS Pathog.*, 6:e1001090.

Kramer, S., Marnef, A., Standart, N. & Carrington, M. 2012. Inhibition of mRNA maturation in trypanosomes causes the formation of novel foci at the nuclear periphery containing cytoplasmic regulators of mRNA fate. *J. Cell Sci.*, 125 (12):2896–2909.

Kramer, S. & Carrington, M. 2011. Trans-acting proteins regulating mRNA maturation, stability and translation in trypanosomatids. *Trends Parasitol.*, 27:23–30.

Kramer, S., Queiroz, R., Ellis, L., Webb, H., Hoheisel, J. D., Clayton, C. & Carrington, M. 2008. Heat shock causes a decrease in polysomes and the appearance of stress granules in trypanosomes independently of eIF2(alpha) phosphorylation at Thr169. *J. Cell Sci.*, 121:3002–3014.

Lamontagne, J. & Papadopoulou, B. 1999. Developmental regulation of spliced leader RNA gene in *Leishmania donovani* amastigotes is mediated by specific polyadenylation. *J. Biol. Chem.*, 274:6602–6609.

Levy, G. V., Banuelos, C. P., Nittolo, A. G., Ortiz, G. E., Mendiondo, N., Moretti, G., Tekiel, V. S. & Sanchez, D. O. 2015. Depletion of the SR-related protein TbRRM1 leads to cell cycle arrest and apoptosis-like death in *Trypanosoma brucei*. *PLoS ONE*, 10:e0136070.

Liang, X. H., Haritan, A., Uliel, S. & Michaeli, S. 2003. Trans and cis splicing in trypanosomatids: mechanism, factors, and regulation. *Eukaryot. Cell*, 2:830–840.

Lin, S., Coutinho-Mansfield, G., Wang, D., Pandit, S. & Fu, X. D. 2008. The splicing factor SC35 has an active role in transcriptional elongation. *Nat. Struct. Mol. Biol.*, 15:819–826.

Manger, I. D. & Boothroyd, J. C. 1998. Identification of a nuclear protein in *Trypanosoma brucei* with homology to RNA-binding proteins from cis-splicing systems. *Mol. Biochem. Parasitol.*, 97:1–11.

Manger, I. D. & Boothroyd, J. C. 2001. Targeted disruption of an essential RNA-binding protein perturbs cell division in *Trypanosoma brucei*. *Mol. Biochem. Parasitol.*, 116:239–245.

Maree, J. P., Povelones, M. L., Clark, D. J., Rudenko, G. & Patterton, H. G. 2017. Well-positioned nucleosomes punctuate polycistronic pol II transcription units and flank silent VSG gene arrays in *Trypanosoma brucei*. *Epigenetics Chromatin*, 10:14.

Melville, S. E., Leech, V., Gerrard, C. S., Tait, A. & Blackwell, J. M. 1998. The molecular karyotype of the megabase chromosomes of *Trypanosoma brucei* and the assignment of chromosome markers. *Mol. Biochem. Parasitol.*, 94:155–173.

Montagna, G. N., Donelson, J. E. & Frasch, A. C. 2006. Procyclic *Trypanosoma brucei* expresses separate sialidase and trans-sialidase enzymes on its surface membrane. *J. Biol. Chem.*, 281:33949–33958.

Moretti, N. S. & Schenkman, S. 2013. Chromatin modifications in trypanosomes due to stress. *Cell. Microbiol.*, 15:709–717.

Naftelberg, S., Schor, I. E., Ast, G. & Kornblihtt, A. R. 2015. Regulation of alternative splicing through coupling with transcription and chromatin structure. *Annu. Rev. Biochem.*, 84:165–198.

Naguleswaran, A., Gunasekera, K., Schimanski, B., Heller, M., Hemphill, A., Ochsenreiter, T. & Roditi, I. 2015. *Trypanosoma brucei* RRM1 is a nuclear RNA-binding protein and modulator of chromatin structure. *MBio*, 6:e00114.

Nilsson, D., Gunasekera, K., Mani, J., Osteras, M., Farinelli, L., Baerlocher, L., Roditi, I. & Ochsenreiter, T. 2010. Spliced leader trapping reveals widespread alternative splicing patterns in the highly dynamic transcriptome of *Trypanosoma brucei*. *PLoS Pathog.*, 6:e1001037.

Ouna, B. A., Nyambega, B., Manful, T., Helbig, C., Males, M., Fadda, A. & Clayton, C. 2012. Depletion of trypanosome CTR9 leads to gene expression defects. *PLoS ONE*, 7:e34256.
Pelle, R. & Murphy, N. B. 1993. Stage-specific differential polyadenylation of mini-exon derived RNA in African trypanosomes. *Mol. Biochem. Parasitol.*, 59:277–286.
Pena, A. C., Pimentel, M. R., Manso, H., Vaz-Drago, R., Pinto-Neves, D., Aresta-Branco, F., Rijo-Ferreira, F., Guegan, F., Pedro Coelho, L., Carmo-Fonseca, M., Barbosa-Morais, N. L. & Figueiredo, L. M. 2014. *Trypanosoma brucei* histone H1 inhibits RNA polymerase I transcription and is important for parasite fitness in vivo. *Mol. Microbiol.*, 93:645–663.
Perales, R. & Bentley, D. 2009. "Cotranscriptionality": the transcription elongation complex as a nexus for nuclear transactions. *Mol. Cell*, 36:178–191.
Pfaffl, M. W., Horgan, G. W. & Dempfle, L. 2002. Relative expression software tool (REST) for group-wise comparison and statistical analysis of relative expression results in real-time PCR. *Nucleic Acids Res.*, 30:e36.
Ramakers, C., Ruijter, J. M., Deprez, R. H. & Moorman, A. F. 2003. Assumption-free analysis of quantitative real-time polymerase chain reaction (PCR) data. *Neurosci. Lett.*, 339:62–66.
Reynolds, D., Cliffe, L., Forstner, K. U., Hon, C. C., Siegel, T. N. & Sabatini, R. 2014. Regulation of transcription termination by glucosylated hydroxymethyluracil, base J, in *Leishmania major* and *Trypanosoma brucei*. *Nucleic Acids Res.*, 42:9717–9729.
Reynolds, D., Hofmeister, B. T., Cliffe, L., Alabady, M., Siegel, T. N., Schmitz, R. J. & Sabatini, R. 2016. Histone H3 variant regulates RNA polymerase II transcription termination and dual strand transcription of siRNA loci in *Trypanosoma brucei*. *PLoS Genet.*, 12:e1005758.
Romero-Meza, G., Velez-Ramirez, D. E., Florencio-Martinez, L. E., Roman-Carraro, F. C., Manning-Cela, R., Hernandez-Rivas, R. & Martinez-Calvillo, S. 2017. Maf1 is a negative regulator of transcription in *Trypanosoma brucei*. *Mol. Microbiol.*, 103:452–468.
Schulz, D., Zaringhalam, M., Papavasiliou, F. N. & Kim, H. S. 2016. Base J and H3.V regulate transcriptional termination in *Trypanosoma brucei*. *PLoS Genet.*, 12:e1005762.
Siegel, T. N., Gunasekera, K., Cross, G. A. & Ochsenreiter, T. 2011. Gene expression in *Trypanosoma brucei*: lessons from high-throughput RNA sequencing. *Trends Parasitol.*, 27:434–441.
Siegel, T. N., Hekstra, D. R., Kemp, L. E., Figueiredo, L. M., Lowell, J. E., Fenyo, D., Wang, X., Dewell, S. & Cross, G. A. 2009. Four histone variants mark the boundaries of polycistronic transcription units in *Trypanosoma brucei*. *Genes Dev.*, 23:1063–1076.
Simarro, P. P., Cecchi, G., Franco, J. R., Paone, M., Diarra, A., Ruiz-Postigo, J. A., Fevre, E. M., Mattioli, R. C. & Jannin, J. G. 2012. Estimating and mapping the population at risk of sleeping sickness. *PLoS Negl. Trop Dis.*, 6:e1859.
Srivastava, A., Badjatia, N., Lee, J. H., Hao, B. & Gunzl, A. 2017. An RNA polymerase II-associated TFIIF-like complex is indispensable for SL RNA gene transcription in *Trypanosoma brucei*. *Nucleic Acids Res.*, 46:1695–1709.
Stanne, T. M., Narayanan, M. S., Ridewood, S., Ling, A., Witmer, K., Kushwaha, M., Wiesler, S., Wickstead, B., Wood, J. & Rudenko, G. 2015. Identification of the ISWI chromatin remodeling complex of the early branching eukaryote *Trypanosoma brucei*. *J. Biol. Chem.*, 290:26954–26967.
Stanne, T. M. & Rudenko, G. 2010. Active VSG expression sites in *Trypanosoma brucei* are depleted of nucleosomes. *Eukaryot. Cell*, 9:136–147.
Ullu, E. & Tschudi, C. 1990. Permeable trypanosome cells as a model system for transcription and trans-splicing. *Nucleic Acids Res.*, 18:3319–3326.
Uzureau, P., Daniels, J. P., Walgraffe, D., Wickstead, B., Pays, E., Gull, K. & Vanhamme, L. 2008. Identification and characterization of two trypanosome TFIIS proteins exhibiting particular domain architectures and differential nuclear localizations. *Mol. Microbiol.*, 69:1121–1136.
Vanhamme, L. & Pays, E. 1995. Control of gene expression in trypanosomes. *Microbiol. Rev.*, 59:223–240.
Wedel, C., Forstner, K. U., Derr, R. & Siegel, T. N. 2017. GT-rich promoters can drive RNA pol II transcription and deposition of H2A.Z in African trypanosomes. *EMBO J.*, 36:2581–2594.
Wright, J. R., Siegel, T. N. & Cross, G. A. 2010. Histone H3 trimethylated at lysine 4 is enriched at probable transcription start sites in *Trypanosoma brucei*. *Mol. Biochem. Parasitol.*, 172:141–144.
Zhou, J., Fan, J. Y., Rangasamy, D. & Tremethick, D. J. 2007. The nucleosome surface regulates chromatin compaction and couples it with transcriptional repression. *Nat. Struct. Mol. Biol.*, 14:1070–1076.

SUPPORTING INFORMATION

Additional supporting information may be found online in the Supporting Information section at the end of the article.

Figure S1. Chromosomal location of primers used for *trans*-splicing assay.
Figure S2. Schematic portion of chromosome 9 containing the PTU-TbNOP86 and ChIP-Seq data of histone H2AZ, H2BV and H4K10ac enrichment regions.
Figure S3. Percentage of Biotin-CTP incorporation in parasites treated or not with Act-D assayed in three genes belonging to the PTU-TbNOP86.
Figure S4. Plots for the Pearson correlation coefficient between experiments for the analyzed regions located in the PTU-TbNOP86.
Figure S5. Precursor and mature mRNA levels were significantly reduced after TbRRM1 depletion.
Figure S6. Transcription factors mRNA levels remain unaffected after *TbRRM1* knockdown.
Figure S7. RTqPCR Cq values of genes used as endogenous control and validation of biotin-CTP incorporation assays.
Table S1. Oligonucleotide sequences.
Table S2. Proportion of BrU positive cells after transcription assays by FACS.